Available online at www.sciencedirect.com
SCIENCE DIRECT®
Journal of Magnetic Resonance 172 (2005) 312–323
JMR Journal of Magnetic Resonance
www.elsevier.com/locate/jmr

An advanced EPR stopped-flow apparatus based on a dielectric ring resonator

Günter Lassmann*, Peter Paul Schmidt, Wolfgang Lubitz

Max Planck Institute for Bioinorganic Chemistry, D-45413 Mülheim/Ruhr, Germany

Received 6 July 2004; revised 14 October 2004
Available online 7 December 2004

Abstract

A novel EPR stopped-flow accessory is described which allows time-dependent cw-EPR measurements of rate constants of reactions involving paramagnetic species after rapid mixing of two liquid reagents. The EPR stopped-flow design represents a state-of-the-art, computer controlled fluid driving system, a miniresonant EPR structure with an integrated small ball mixer, and a stopping valve. The X-band EPR detection system is an improved version of that reported by Sienkiewicz et al. [Rev. Sci. Instr. 65 (1994) 68], and utilizes a resonator with two stacked ceramic dielectric rings separated by a variable spacer. The resonator with the mode TE(H)$_{011}$ is tailored particularly for conditions of fast flowing and rapidly stopped aqueous solutions, and for a high time resolution. The short distance between the ball mixer and the small EPR active volume (1.8 μl) yields a measured dead time of 330 μs. A compact assembly of all parts results in minimization of disturbing microphonics. The computer controlled driving system from Bio-Logic with two independent stepping motors was optimized for EPR stopped-flow with a hard-stop valve. Performance tests on the EPR spectrometer ESP 300E from BRUKER using redox reactions of nitroxide radicals revealed the EPR stopped-flow accessory as an advanced, versatile, and reliable instrument with high reproducibility.

Keywords: Cw-X-band EPR; Stopped-flow kinetics; Dielectric resonator; Time sweep; Rate constants

1. Introduction

A stopped-flow (SF) experiment with EPR detection allows the observation of a time-dependent change of the amplitude of an EPR signal at a distinct field value (usually at the maximum of first derivative) during the reaction of two reactants in the liquid state by time-sweep acquisition (kinetic display). The result of such a measurement is a rate constant for formation, decay, or conversion of a paramagnetic species, e.g., a radical occurring in the reaction mixture. The procedure is analogous to the well-established case of stopped-flow operation with optical detection in which a time-dependence of the optical absorption at a distinct wavelength is observed.

Typical applications of EPR stopped-flow (EPR-SF) instruments have been reported in chemistry and biochemistry, and the kinetics of transient radicals occurring in typical redox reactions with life-times down to milliseconds have been published. Examples are the decay of stable nitroxide radicals during reduction by ascorbate [1–3] or dithionite [4], and formation and decay of semi-dehydro ascorbate radicals during the oxidation of ascorbate by Ce^{4+} [5,1]. Radicals that are not EPR-detectable in the liquid state due to short relaxation times T_1 (linewidth broadening), as e.g., hydroxyl ($OH^{\bullet}$), superoxide ($O_2^{\bullet -}$), or alkyl thiyl ($R–S^{\bullet}$), cannot be studied directly by EPR-SF techniques. Nevertheless, the spin-adducts of these radicals with nitrones, yielding nitroxide-type radicals, are EPR-active and their

* Corresponding author. Fax: +49 208 306 3951.
E-mail address: lassmann@mpi-muelheim.mpg.de (G. Lassmann).

1090-7807/$ - see front matter © 2004 Elsevier Inc. All rights reserved.
doi:10.1016/j.jmr.2004.10.015

kinetics can be monitored also by EPR-SF [6,7]. The kinetics of reduction of a protein-associated tyrosine radical in the R2 protein of *Escherichia coli* and mouse ribonucleotide reductase (RNR) by inhibitor-based reductants, as hydroxyurea [8] and *para*-alkoxyphenols [9], have been investigated. In R2 mutants of *E. coli* RNR the life-times of transient tryptophan radicals were determined by EPR-SF [10]. Using nitroxide radicals, kinetics of conformational changes (folding and unfolding of proteins) in spin-labeled proteins (via line shape changes of the EPR spectra) [3,4,11,12], and the kinetics of diffusion of lipid-like spin-probes in biomembranes have been reported [13,14]. In cases where paramagnetic transition metal ions or their complexes are EPR-active in the liquid state, due to sufficiently long spin–lattice relaxation times, the kinetics of a valence change or a spin-state change upon redox reactions, or the kinetics of a ligand exchange, can also be studied by EPR-SF technique, see, e.g. [15].

Stopped-flow instruments with optical detection have been established since 1952 [16], SF techniques with EPR detection have first been introduced in 1960 [17]. EPR-SF accessories with improved driving systems are available since 1980; respective data are summarized in Table 1. The progress in the field and the limitations will be briefly discussed in the following.

The SF instrument described by Klimes et al. [5] employed a conventional rectangular waveguide H_{102} resonator with a large sample volume and a rather large dead volume (the volume between mixer and EPR-active region). This is unfavorable for a high time resolution, but was partly compensated in this set-up by a high flow-rate, a pressure-resistive EPR cell, and a hard-stop valve leading to a time resolution of about 1 ms. The driving unit consisted of two strong stroke magnets which allowed a fast pulsed drive, but only with a fixed volume and a constant high flow-rate. Another limitation was the extreme sensitivity of waveguide resonators against mechanical shocks, which produce large artificial peaks in the EPR time sweep (microphonics) and often occur under SF operation conditions.

Substantial progress in EPR-SF technology came from two different technical developments. A new driving system from UPDATE Instruments (Wisconsin, USA), using a microprocessor controlled powerful stepping motor, allowed the adjustment of a precise flow of different volumes at variable rates. Another major advantage came from the development of new microwave resonance structures, i.e., loop gap and dielectric ring resonators that avoid waveguide parts. Both of these types of resonators are much smaller as waveguide resonators and can easier be designed and adapted to the requirement of fast SF techniques, i.e., a short distance between mixer and EPR detection cell. The EPR-SF accessories listed in Table 1 benefited from both of these innovations [1,2,4].

The loop gap resonator of Hubbel et al. [1] published in 1987 exhibited a very small EPR sample volume and is well-designed for a probe-head of an EPR-SF accessory using a Wiskind grid mixer and the UPDATE driving unit; the achieved dead time was ca. 4 ms.

The EPR-SF instrument reported by Sienkiewicz et al. in 1994 [2,3] utilized a dielectric ring resonator which exhibited favorable properties for EPR-SF operation, e.g., a 10 times higher Q factor, and lower microphonics than a loop gap resonator. The construction is based on detailed calculations of the microwave properties of dielectric ring EPR resonators made of zirconium titanate ceramics [(Zr, Sn)TiO_4] [18]. Rutile (TiO_2) has also been used for dielectric ring EPR resonators due to its large dielectric constant ($\varepsilon = 100$) [19], but the temperature coefficient of the resonance frequency of rutile is unfavorably larger by a factor of about 1000 than that of zirconium titanate [20]. Therefore, (Zr, Sn)TiO_4 ceramics have been preferred for microwave resonators for various EPR purposes [18,21], although impurities from Fe^{3+} contaminations may lead to small, rather broad background EPR signals [21]. Single dielectric ring resonators of zirconium titanate exhibit an unloaded Q of 5300 at room temperature, and remarkable large Q values at very low temperatures (26,000 at 4.2 K, and 1×10^6 at 1.4 K [20]).

The resonator employed in [2,3] contained *two* stacked dielectric rings with a spacer between them, so that the frequency could be varied by the thickness of the spacer by about 1 GHz. The smaller size of the EPR-active volume in comparison with the standard waveguide H_{102} cavity together with a higher H_1 field and an almost absent E field at the sample position in the dielectric resonator, allowing a higher filling factor, led to a considerable enhancement of the sensitivity by a factor of about 30, particularly for small samples of aqueous solution, e.g., of nitroxide radicals or Mn^{2+} [2,20,21]. Furthermore, the small size of dielectric rings and their small EPR volume allowed a close distance to the mixer, which led to a dead time of only 1.6 ms reported in [2].

The EPR-SF accessory of Grigoryants et al. [4] reported in 2000 is similar in construction to that in [2], but utilizes a highly sophisticated micro ball mixer embedded in a quartz capillary that is intimately fused to the EPR sample tube. The very short distance between mixer and EPR-active volume and the corresponding smaller dead volume as well as the narrower sample tube led to a very short dead time (Table 1), which has been deduced from geometrical data and from reaction of a nitroxide spin probe with dithionite [4]. The very thin wall of the EPR sample tube (0.075 mm) and the fragile quartz mixer, however, would not be sufficiently resistive against the pressure pulse of a hard-stop valve.

Table 1
Technical data of the X-band EPR stopped-flow apparatus and comparison with previous techniques[a]

Technical properties	Klimes et al.[b] [5]	Hubbel et al. [1]	Sienkiewicz et al. [2]	Grigoryants et al. [4]	This work (2004)
Reactant driving system	Two stroke-magnets, pulse-shaped drive	Update ram: one strong step motor	Update ram: one strong step motor	Update ram: one strong step motor	BioLogic MIXCON: Two step motors
Maximal flow-rate	25 ml/s, fix	5.2 ml/s, variable	5 ml/s, variable	3.3 ml/s, variable	5 ml/s, variable
Hard-stop valve	Solenoid valve	—	—	—	Solenoid valve
Software for driving system	—	—	—	—	Windows PC-based
Type of mixer	Four tangential yets in two areas, opposite direction	Wiskind grid mixer	Wiskind grid mixer	Micro quartz capillary mixer	Berger ball mixer
Type of resonator	Rectangular waveguide cavity H_{102}	Loop gap	Two dielectric rings (with spacer)	Two dielectric rings (without spacer)	Two dielectric rings (with spacer)
EPR sample tube					
i.d. (mm)	1.3	0.53	0.60	0.40	0.60
o.d. (mm)	7.3	0.70	0.84	0.55	1.26
Wall thickness (mm)	3.0	0.085	0.12	0.075	0.33
EPR-active volume (μl)	28	1.2	2.0	0.5	1.8
Loaded Q	1800	100	1100	1000	1400
Distance					
Mixer-EPR entrance (mm)	12	18	9.1	2	5
Mixer-EPR center (mm)	25	21	12.6	4	8
Dead volume (EPR center) (μl)	20	6.2	8	0.5	1.6
Dead time (EPR center) (ms)	1 (with hard stop)	4	1.6	0.15[c]	0.33
EPR data acquisition	VARIAN E3, BRUKER ESP-300E	VARIAN E102	BRUKER ER-200D	BRUKER ER-200D	BRUKER ESP-300E
Thermostating of reactants	—	x	x	x	x

[a] Techniques with pneumatical drive are not included, see citations in [1].
[b] Data refer to an improved instrument in comparison to those in [5] which was produced in 1983–1990 in the Institute of Scientific Instruments, Berlin–Adlershof, which was applied in [8–10,13–15].
[c] A shorter dead time of 0.065 ms was given for this apparatus in [12].

Generally, we oriented the design of our EPR-SF accessory on the instrument documented in [2], which used a frequency-adjustable dielectric ring resonator. We designed our instrument especially for robust conditions of SF operation. The Berger ball mixer, which allows a closer distance to the EPR cell, was preferred because of its smaller size compared to the Wiskind grid mixer. Additionally, we employed a hard-stop valve and the completely software-controlled MIXCON II driving unit (BioLogic, Grenoble, France) after an adaptation for EPR-SF operation. Thus, the EPR-SF accessory, reported here, represents an advanced instrument combining the progress of leading EPR techniques and modern rapid flow technologies, combined with direct fast data collection in the rapid acquisition channel of the EPR spectrometer ESP 300E. Most parts of the instrument are commercially available.

2. Technical description of the dielectric resonator-based EPR stopped-flow accessory

The dielectric resonator-based EPR-SF accessory includes two instrumental parts, a MIXCON II apparatus (BioLogic, Grenoble, France) for driving of liquid reactants and the EPR detection system developed in our institute. A block diagram of the entire instrument is shown in Fig. 1.

2.1. MIXCON driving unit and redesign for EPR stopped-flow operation

The MIXCON II apparatus was originally constructed for freeze-quenching (FQ) operation. The driving unit consists of two driving syringes (**DS1**, **DS2**), which are driven by two independent stepping motors

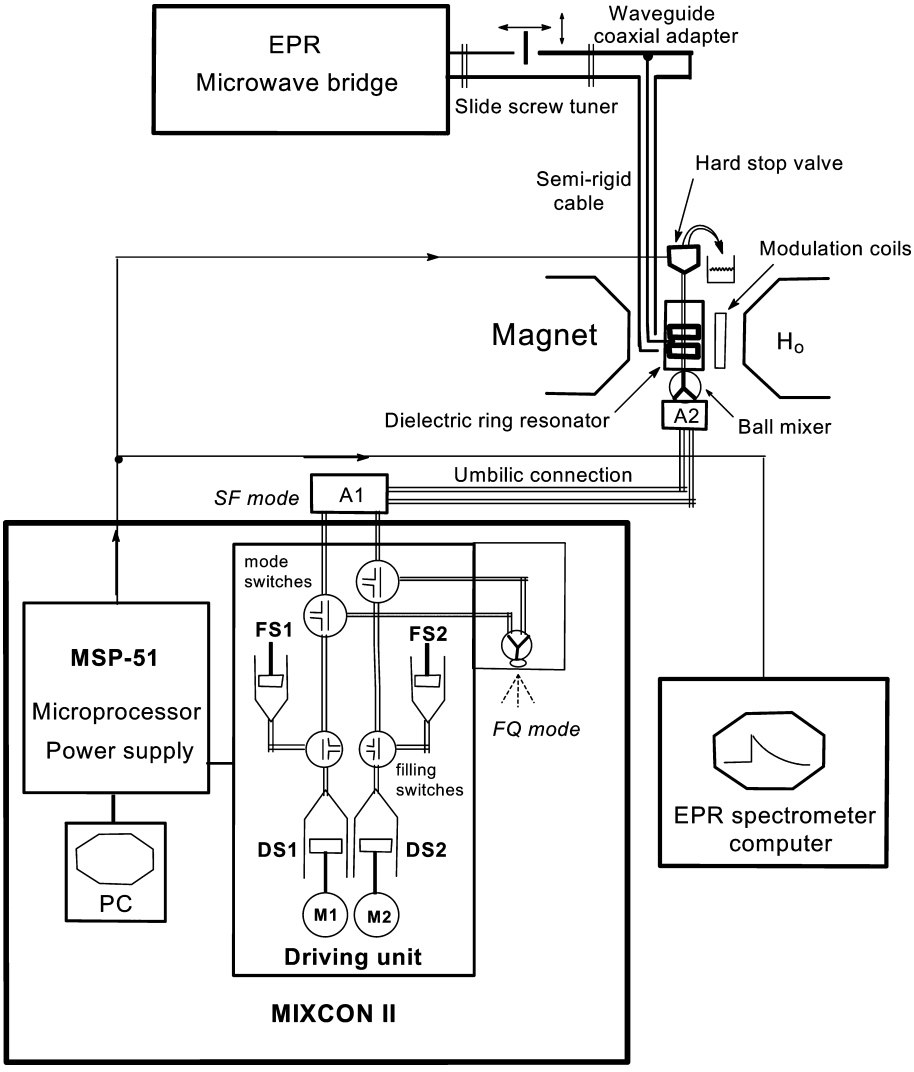

Fig. 1. Block diagram of the dielectric resonator-based EPR stopped-flow system, **DS**, driving syringe; **FS**, filling syringe; and **M**, stepping motor, for explanations see text.

(**M1**, **M2**) controlled electronically by the microprocessor-based power supply MPS-51 (Fig. 1). The stainless steel syringes (each 4.5 ml) and the stepping motors allow maximal flow-rates of 4 ml/s per syringe. The driving syringes are loaded via two 3-way valves (filling switches) from two filling syringes (**FS1**, **FS2**). A software package based on Microsoft Windows 3.1, running on a PC, controls via the MPS-51 unit the operation of the driving unit with programs, e.g., for filling of syringes, choice of shot volume and shot time, i.e., flow-rate, and mixing ratio (from 1:1 up to 1:10), and for the display of filling level, available number of shots, and shooting operation. The software package (SF Module Application Driving Software V 1.10) can be used also for SF operation, e.g., for triggering of a kinetic display, activating the hard-stop valve, and repeated shooting in case of data accumulation.

For use in EPR-SF operation the MIXCON driving unit needed some technical redesign. The dielectric resonator and the closely assembled separate mixer are localized between the poles of an electromagnet and need a distance of 80 cm to the driving unit. Thus, a new tubing link between the resonator and the driving unit and another output in the driving unit (additionally to those for the FQ-mixer/nozzle) is required for the two liquid components. This link, the so-called ''umbilic cord,'' contains two connecting hoses and two adaptors, one (**A1**) to the new outlet at the driving unit, and the other one (**A2**) to the mixer/adaptor of the EPR detection system (Fig. 1). Two new pressure-resistant valves (4-port switching valve, Type: V-101L, made of PEEK, from Upchurch Scientific, Oak Harbour, WA, USA) have been installed in the thermostating chamber of the driving unit. These valves allow an easy switching of the two reactants for two alternative operation modes, to the nozzle for freeze-quenching (off-line with the EPR spectrometer for sample preparation), or, via the umbilic cord, to the EPR resonator for EPR-SF (on-line with the EPR spectrometer).

The required new parts for EPR adaptation, as the umbilic cord with the adaptors, the mixer/resonator adaptor, the mixer, and the hard-stop valve were constructed and produced (besides the driving system of the MIXCON II) by BioLogic. The EPR dielectric ring resonator and the adaptation of the driving unit for EPR-SF operation was designed, produced, and tested in our institute.

2.2. Berger ball mixer adapted to the EPR cuvette

Details of the mixer/resonator assembly are shown in Fig. 2. The mixer **23** made of PEEK (polyether-etherketone) is assembled in the mixer/adaptor body (PEEK) **21** that is linked at the entrance to the two connecting PEEK tubes **13** in the umbilic cord adaptor **A2** via a threaded connection **10**. At the outlet side, the mixer/adaptor **21** is connected by six M2 brass screws **20** in counterbores with the holding body **19**, which encloses the dielectric resonator.

The mixer is of the ''ball-type,'' described first in 1968 by Berger et al. [22]. In the mixer, the two reactants flow around a ball-like hemi-sphere and enter only a few millimeters behind the ball a region of intense turbulence, which provides a high mixing efficiency. A complete mixing of the reactants shortly after the mixer exit is necessary for SF experiments with a high time resolution. The used mixer was constructed by BioLogic, the design is close to that shown in [22]. The robust mixer has cylindrical shape (5 mm o.d. and 5 mm height) and is sealed by two O-rings of silicon rubber (Viton), the lower one **8b** (1.2 mm i.d. and 1.5 mm thickness) seals the mixer entrance and the upper one **8a** (1.0 mm i.d. and 2.0 mm thickness) seals the mixer outlet and the entrance part of the EPR capillary. A shortest possible distance of 5 mm between the mixer and the EPR-active sample volume (see also Fig. 3) has been designed, which is a prerequisite for a high time resolution of the entire instrument. As shown in Fig. 5, incomplete mixing occurs for flow-rates $\leqslant$2 ml/s. The turbulence region behind the mixer exit (1–2 mm for low viscous liquids and medium flow rates [22]), the O-ring PEEK fitting elements for the capillary **22** (1.5 mm), the lower shielding lid **1b** (copper disc, 0.5 mm), and the lower distance ring **2c** (Rexolite, 1 mm) are found within this distance (Fig. 2). The ball-mixer can easily be disassembled from the mixer/adaptor unit for cleaning or replacement.

2.3. EPR detection system

2.3.1. Properties and assembly of the dielectric ring resonator

The dielectric ring resonator (**R** in Fig. 2) is the essential part in the EPR detection system of the EPR-SF accessory. Two dielectric rings **3** and the Rexolite spacers **2a**, **2b**, and **2c** are located inside a cylindrical resonator body **7** that is also made from Rexolite. The resonator body is enclosed by a microwave shield, to prevent microwave radiation and to get a high Q factor of the resonator. The cylindrical part of the shield **4** is made from a silver foil (30 μm thickness),[1] and the two circular lids are copper discs of 0.5 mm each (**1a**, **1b)**.

A quartz capillary used as EPR sample tube **18** is localized in the long axis of the dielectric rings (see also Section 2.3.3).

[1] The silver foil shields the high frequency modulation field of 100 kHz to some extent so that we preferred lower modulation frequencies. For each frequency used a calibration of the modulation field at the EPR sample was performed (see Section 3.1).

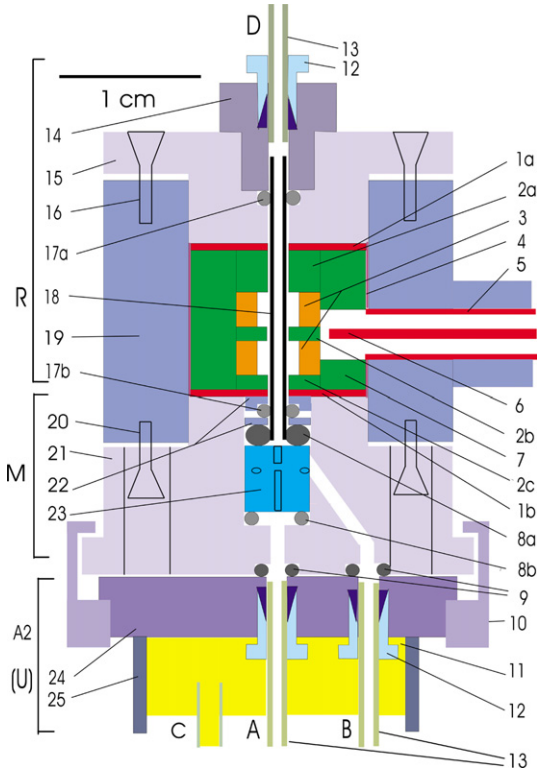

Fig. 2. Details of the EPR detection system: Assembly of dielectric ring resonator (**R**), mixer-resonator adaptor (**M**), and umbilic cord adaptor (**A2**) of the EPR stopped-flow apparatus; section through the assembly parallel to the axis of the EPR sample tube; (**A**) and (**B**): inlet of the two reactants from the driving syringes; (**C**): inlet tube of the thermostating coolant in the umbilic cord; (**D**): exit of the reacted mixture and connection to the hard-stop valve (see Fig. 1). **1** (copper disc) upper **(a)** and lower **(b)** microwave shielding lid (red); **2** (Rexolite) upper (a), middle (b), and lower (c) spacer discs (green); **3** (zirconium titanate) dielectric rings (orange); **4** (30 μm silver foil) microwave shield (magenta); **5** semi-rigid coax microwave cable (red); **6** coupling loop (side view) and middle wire of the coax cable (red); **7** (Rexolite) cylindrical resonator body (green); **8** (viton) upper **(a)** and lower **(b)** O-ring for mixer compression seals (dark and light gray); **9** (Viton) compression O-ring seals for the two reactant lines at the interface between the umbilic cord adaptor (**A2**) and the mixer/resonator adaptor (**M**) (dark gray); **10** (Kel-F) threaded connection linking the umbilic cord (**U**) and the mixer/resonator adaptor (M) (violet); **11** thermostating coolant in the umbilic cord (yellow); **12** threaded compression fitting (from ABIMED or SUPELCO) for PEEK hoses (light blue); **13** (PEEK) hose tubings for the reactants and the mixture (gray-green); **14** (Kel-F) threaded compression seal for upper capillary O-ring (violet); **15** (Kel-F) upper lid of the resonator containing capillary fitting and outlet PEEK tube (light violet); **16** (brass) M2 screws (six equally spaced) for connecting the upper lid with the resonator holder; **17** (Viton) upper **(a)** and lower **(b)** O-rings for positioning and sealing of the capillary (gray); **18** (suprasil quartz) EPR sample tube capillary (black); **19** (Kel-F) resonator holding body (gray-blue); **20** (brass) M2 screws (six equally spaced) for compressing the O-rings of the mixer and the lower capillary O-ring; **21** (Kel-F) lower lid of the resonator and mixer/resonator adaptor (M) carrying the mixer (light violet); **22** (Kel-F) compression seal elements for lower capillary O-ring and upper mixer O-ring (gray-blue); **23** (Kel-F) ball mixer (blue); **24** umbilic cord terminus (**A2**) connecting the mixer/adaptor (**M**) (dark violet); **25** folded flexible wall of the umbilic cord (dark-blue).

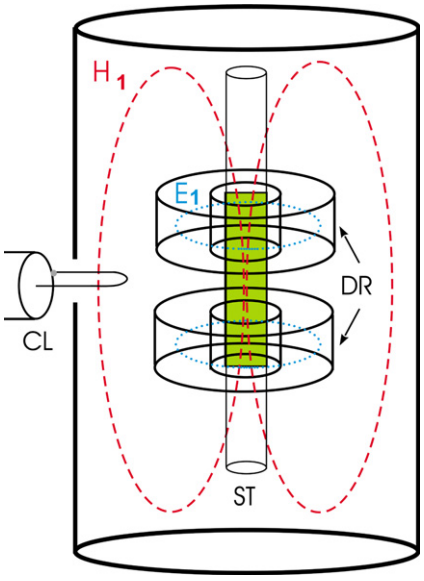

Fig. 3. Distribution of the microwave wave E_1 and H_1 fields within the dielectric ring resonator in the symmetrical cylindrical TE$(H)_{011}$ mode; **DR** dielectric rings, **ST** sample tube, EPR active volume in green, **CL** coupling loop, **bold frame** microwave shield, $\mathbf{H_1}$ microwave magnetic field (red dashed line), $\mathbf{E_1}$ microwave electric field (blue dotted line). Rexolite spacers and the cylindrical resonator body have been omitted for clarity.

The Q factor of the resonator depends on the radius of the center hole of the dielectric rings, the geometry of the coupling hole, the conduction loss of the displacement currents in the cylindrical shield, and on the dielectric loss of the material inside the resonator. The material of the dielectric rings **3** is zirconium titanate ceramics, type: S/ME (from MuRata-Erie North America, R/F microwave products, State College Pennsylvania) with $\varepsilon = 30$ and $\mathrm{tg}\delta = 8.3 \times 10^{-5}$ at 8 GHz [2,20,21]. Rexolite is a polystyrene polymer with a small dielectric constant ($\varepsilon = 2.6$) and a low dielectric loss ($\mathrm{tg}\delta = 6.6 \times 10^{-4}$) [2], which leads to a focusing of the electric microwave field component mainly in the dielectric rings with the higher ε favoring a high Q factor. Thus, the volume of the resonator inside the microwave shields **4** and **1** is mainly filled with Rexolite and the two ceramic rings. All parts are packed tightly to a compact assembly compressed by the two lids **15** and **21**, which guarantees low microphonics upon SF operation.

The resonance frequency of a single dielectric ring is primarily determined by its geometrical size and usually has a fixed value. An elegant method to change the resonance frequency, however, is the use of two stacked rings with variable distance [2,18]. This principle was adopted also in our construction. The position of the rings inside the body is fixed by a lower **2c**, a middle **2b**, and an upper **2a** distance spacer disc (Fig. 2). The thickness of **2b** was selected according to the required range of resonance frequencies.

The dielectric resonator was especially designed for a closest possible distance (5 mm) between the center of the EPR-active volume and the mixer exit, which is required for a high time-resolution. Therefore, the dielectric rings were positioned only 1 mm (lower Rexolite spacer **2c**) above the lower shielding copper lid **1b**, this, however, leads to an asymmetry of the resonator (Fig. 2). Measurements using a microwave sweeper (Signal generator, type: SMR-40, 1–40 GHz, from Rhode and Schwarz, Munich, Germany) have shown, that in this case the resonance frequency of the resonator is enhanced by 100 MHz, but the Q factor is not decreased. The fastest volume flow-rate of the driving unit, which allows reproducible shots with a volume of 150 μl, is 5 ml/s through the EPR cell. The dead volume of 1.4 μl estimated from the geometry between the mixer exit and the EPR-active volume yields a dead time of 0.28 ms at the flow rate of 5 ml/s.

The microwave sweeper has been used to measure the resonance frequency and the loaded and unloaded Q factors of the dielectric ring resonator, as well as to optimize the shape and size and the penetration depth of the coupling loop and to test the performance of the slide screw tuner as a variable coupling element. To cover the frequency range of the BRUKER ESP 300E EPR spectrometer (9.03–9.98 GHz), we have designed our resonator with two identical stacked cylindrical dielectric rings of 6.0 mm o.d., 3.0 mm i.d., and 2.6 mm height each; the thickness of the spacer **2b** is 1 mm (Fig. 2). Here, the resonance frequency is 9.83 GHz and the EPR-active length (approximately twice the height of the rings plus the spacer-distance) (Fig. 2) is 6.2 mm, which corresponds to a sample volume of 1.8 μl. The Q factors are about 2500 in case of an empty quartz capillary (unloaded), and 1400 for a capillary filled with water (loaded). Characteristic data of the resonator/mixer assembly are summarized in Table 1.

The microwave mode of the dielectric ring resonator is TE$(H)_{011}$ (Fig. 3), and exhibits a field distribution which is similar to that of the cylindrical TE$(H)_{011}$ waveguide cavity [2,18]. The electric field is localized predominantly inside the dielectric rings as concentric circles, the toroid-like magnetic field has a maximum at the long axis of the two stacked dielectric rings where the EPR quartz capillary with the liquid sample is positioned. For two stacked and coupled dielectric rings with a certain distance, two different microwave modes are possible, an asymmetrical TE$(H)_{012}$ mode with individual H field lobes around each ring, and a symmetrical TE$(H)_{011}$ mode with a common lobe around both rings [19], as shown in Fig. 3. The asymmetrical TE$(H)_{012}$ mode has a H_1 field node in the center of the resonator and is not useful for our purpose. Since the EPR-relevant TE$(H)_{011}$ mode has a lower frequency than the asymmetrical one [19], it can easily be recognized by using a microwave sweeper. Furthermore, the position of the coupling loop between the two dielectric rings favors excitation of the symmetrical mode.

2.3.2. Coupling of the dielectric ring resonator to the microwave bridge

The microwave is coupled magnetically (H_1 field) to the resonator by a loop formed from the internal wire of the semi-rigid coaxial cable, whose area is coplanar with the area of the dielectric rings and excites the symmetrical TE$(H)_{011}$ mode (Fig. 3). The coupling loop **6** is inserted through a hole in the sidewalls of the resonator shield **4**, the resonator body **7**, and the resonator holder **19**, its distance to the middle spacer **2b** is about 1–2 mm (Fig. 2). An optimal distance of the coupling loop to the dielectric rings is important for a high Q factor; a too close distance lowers the Q, a too far distance complicates a critical coupling. A semi-rigid flexline coaxial cable **5** (o.d. 3.6 mm) connects the resonator with the waveguide of the EPR spectrometer via a waveguide-coaxial adapter (Fig. 1). The coupling of the dielectric resonator can be fine-tuned by a slide screw tuner in the waveguide line that is localized in a distance of about 40 cm from the resonator. The choice of a slide screw tuner in the microwave line as a variable coupling device proved to be a better solution than a tunable short in the coax line close to the resonator. It allows a large range of tuning and a precise adjustment of critical coupling by its fine micrometer drive and avoids movable parts near the resonator, which may cause microphonics. A microwave phase-shifter (with varying position of a dielectricum in the E-field of the waveguide) was also tested as a variable coupling element, but the tuning range proved to be smaller.

2.3.3. EPR cuvette and sealing

Parts having contact with the reactants are made from inert materials as stainless steel (syringes), PEEK and teflon (hoses), quartz (EPR cuvette), and Viton (O-rings). The EPR cuvette is a Suprasil quartz capillary **18** (Quarzschmelze Ilmenau, Germany) (1.26 mm o.d., 0.6 mm i.d., and 31 mm length) which is tightly fixed in the cylindrical axis of the dielectric rings by two O-rings **17a**, **17b** (1.0 mm i.d., 1.5 mm thickness) made of silicon rubber (Viton). These rings serve also as seals for the flowing reactants (Fig. 2). Pressure tightness is required for the entire liquid column, which is temporarily under overpressure produced by the driving shot and the hard-stop valve. The liquid column involves the 3-way valves, the connecting hoses, the mixer, and the quartz capillary. Non-expandable, but flexible pressure-resistant PEEK tubing **13** (1.6 mm o.d., 0.7 mm i.d.) as connecting hoses with corresponding sealing **12** as well as a relatively thick-walled (0.3 mm) quartz EPR tube have been used successfully. The thicker capillary wall is required because of the additional pressure load caused by the hard-stop valve, which was not ap-

plied in previous EPR-SF accessories [1,2,4] that worked with capillary walls ⩽0.1 mm (Table 1). The O-ring seals of the EPR capillary are compressed separately, the upper one **17a** by a threaded compression seal **14**, and the lower one **17b** by six brass screws **20** in the mixer/resonator adaptor **21** (M) which also compress the O-ring seals **8a** and **8b** of the mixer.

2.3.4. Assembly of the entire resonator

All parts of the dielectric resonator are rigidly assembled. The resonator/mixer unit in turn is mounted in a Kel-F block, which also contains the modulation coils. The block is fixed rigidly in the pole gap of the EPR magnet. This block is mechanically linked to the two microwave elements, the waveguide-coax adaptor and the slide screw tuner, by two stiff aluminum tubes. The waveguide flange of the slide screw tuner is connected to the microwave bridge of the EPR spectrometer and the entire resonator assembly can be exchanged for an usual waveguide (or flexline) resonator.

2.4. Hard-stop valve for EPR stopped-flow operation

A high time resolution in SF experiments depends, in addition to the construction of the resonator, on several further conditions. Important for preparing the reactants is to avoid any gas bubbles in the entire liquid column of the apparatus which would cause strong signal spikes upon passing the EPR cuvette. This requires removal of dissolved air from the reactants by degassing, and a careful loading of the driving syringes. Furthermore, a quick and complete stop of the flow is necessary for achieving a sharp time-point for the start of the kinetic decay and the time-sweep display. With an open outlet—even in case of a quick stop of the syringe stepping motors—the inertia of the liquid column may result in a slight after-flow and a rebound of the liquid, which reduces the time resolution, particularly in the millisecond range. To avoid this effect, a hard-stop solenoid valve, first described in [23] and developed recently by the BioLogic Company for SF machines with optical detection, is connected with the exit PEEK hose at the outlet of the EPR flow-resonator (Fig. 1). In any way the system has to be air-free, since an air bubble in the system will be compressed during the shot and will push the liquid column upon expansion after the pressure was released. However, a residual small elasticity of the system remained which is caused by the necessity to use O-ring sealings made of silicon rubber. The hard-stop valve is mounted separately from the resonator assembly on the EPR magnet support. The microprocessor-controlled hard-stop valve interrupts the flow quickly, the closing time of the valve is ⩽2 ms. The MIXCON software allows a setting of the time-point of the valve action to 0–5 ms *before* the driving syringes stop so that the electric signal can be sent to the valve 2 ms before the motors stop to assure that the valve closes at the same time. This option allows to optimize the fast stop of the flowing liquid. In test experiments the function of the hard-stop valve has been shown to be very effective for getting kinetic traces in good quality.

2.5. Thermostating of the reactants

Rate constants of chemical reactions depend sensitively on temperature. Thus, measurements at various temperatures of the reactants are desired. Additionally, proteins as reactants are often not stable enough at room temperature and need investigations at lower temperature. Therefore, the EPR-SF accessory was designed such that a thermostating (cooling) of the reactants is included. The MIXCON II driving unit is equipped with a thermostate chamber, which contains the driving syringes, the 3-way valves for filling and shooting operation, and the mixer/nozzle unit for FQ. This chamber can be connected with a commercial thermostate allowing temperatures for aqueous solutions near 0 °C, and below 0 °C for organic solvent. For the EPR-SF mode, we have redesigned the MIXCON unit with a new pair of output PEEK tubes and two additional pressure resistant 3-way valves that are also localized in the thermostate chamber (Fig. 1).

Adaptor **A1** of the umbilic cord **U** holds two further outlets that are connected to the coolant in the thermostate chamber (details omitted for clarity in Fig. 1). A coolant tube **C** linked to the inlet tube of the thermostate chamber is open at the mixer end **A2** of the umbilic cord **U** (see Fig. 2), so that the whole cord is filled with the thermostated coolant **11** embedding the two PEEK hoses **13** which contain the reactants (Fig. 2). The mixer **23** inside the mixer/adaptor **21**, which is linked to the umbilic cord, is cooled via the material of the adaptor. Thus, all the reactant in the two hoses of the umbilic cord (about 400 µl each) and the driving syringes (**DS** in Fig. 1) are equilibrated with the coolant. The EPR cuvette is not thermostated, but during the short time of a shot and a short observation time the mixture can safely be expected to keep the temperature of the coolant.

3. Functional tests and application of the EPR stopped-flow accessory

3.1. Dielectric ring resonator

The resonance frequency and the unloaded and loaded (water-filled cuvette) Q factors of the dielectric resonator are given and discussed in Section 2.3.1.

Phase optimization and calibration of the modulation channel of the resonator in the EPR spectrometer require a test sample with a single EPR line in the liquid

phase—as DPPH for solid samples. We used the stable sulfonyl radical anion ($SO_2^{\bullet -}$) in aqueous solution as a suitable system. The EPR spectrum of this σ-type radical consists of an intense single line at $g = 2.0057$ with a linewidth of 0.07 mT and four very weak hf satellite lines from the natural ^{33}S isotope of nuclear spin 3/2 with $a_{iso} = 1.42$ mT [24]. The sample preparation is done with a 1 M aqueous solution of sodium dithionite ($Na_2S_2O_4$), in which the dissociation equilibrium: $S_2O_4^{2-} \rightleftharpoons 2SO_2^{\bullet -}$ provides a sufficient radical concentration of $SO_2^{\bullet -}$ that is stable for some hours at room temperature.

The dielectric ring resonator exhibits a weak background EPR signal at room temperature, an asymmetric singlet at $g = 2.010$ with a width of about 1 mT that is noticeable in the inset of Fig. 4a. Its origin was clearly identified as resulting from the ceramics ((Zr, Sn)TiO_4) of the dielectric rings. The signal could come from Fe^{3+} impurities as observed earlier [21], or, as in our case, from the enlargement of the central hole from 2 to 3 mm i.d. using a laser (the ring with 2 mm i.d. did not exhibit this signal). The quartz sample and the Rexolite material inside the resonator were free of background EPR signals at room temperature. Nevertheless, time-swept EPR measurements are not disturbed by this background signal.

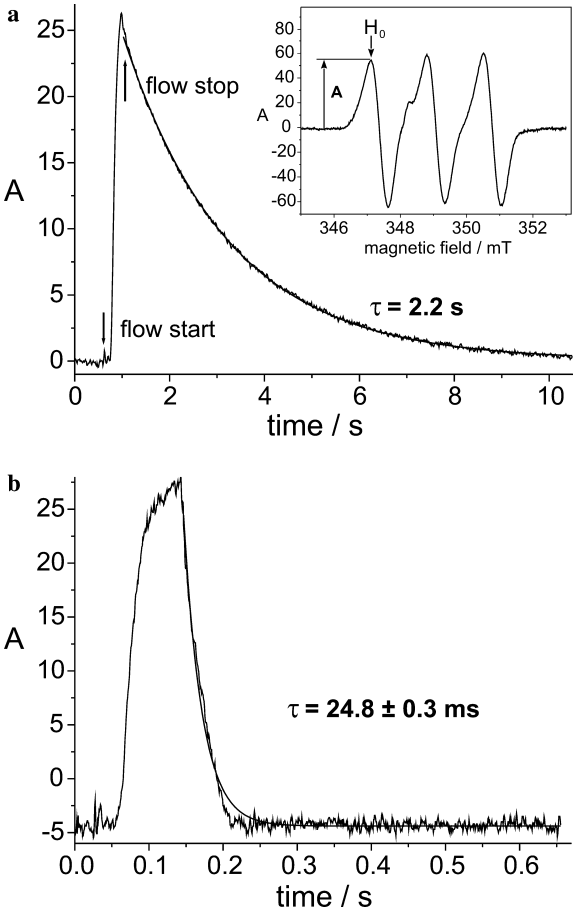

Fig. 4. Operational tests of the EPR stopped-flow apparatus: time dependence of the EPR amplitude at a fixed field in a typical shooting profile during the flow and of the reaction kinetics after stopping the flow (see also text). The decay has been fitted with a single exponential (bold line), the resulting relaxation time τ (the inverse of the reaction rate) is given. (a) TEMPOLE (1 mM) + ascorbate (500 mM), pH 3.0. EPR: 348.5 mT, 0.7 mT (50 kHz), 10 mW, 1.28 ms; flow: 2 × 200 µl, 1.0 ml/s, 600 ms delay time. Inset: EPR spectrum of TEMPOLE (before mixing), field position for kinetic display is marked by a bold arrow. (b) TEMPOLE (1 mM) + dithionite (10 mM), pH 7.0. EPR: 347.1 mT, 0.7 mT (12 kHz), 10 mW, 1.28 ms; flow: 2 × 120 µl, 2.0 ml/s, 20 ms delay time.

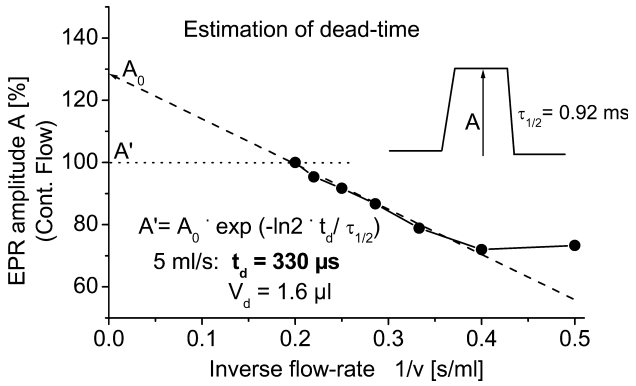

Fig. 5. Experimental estimation of dead-time (t_d) and dead-volume (V_d) of the EPR-SF apparatus. The relative steady-state EPR amplitude A (before the hard-stop) of a rapid reaction (3 mM TEMPOLE and 500 mM dithionite) is plotted versus the inverse flow-rate. Inset: scheme of the shooting profile showing the continuous-flow EPR amplitude A and the half-life time $\tau_{1/2}$ (0.9 ms) of the reaction (see also Fig. 6). EPR: 346.4 mT, 0.45 mT (50 kHz), 10 mW, scan time: 512 ms, time constant: 2.56 ms; (for estimation of $\tau_{1/2}$: scan time, 154 ms; time constant, 0.16 ms). Flow: 2 × 150 µl, 2–5 ml/s.

3.2. Performance of the EPR stopped—flow accessory

Tests of the function of the EPR-SF accessory under flow conditions have been performed using the chemical reduction of the stable nitroxide radical 4-hydroxy-2,2,6,6-tetra-methyl-piperidine-*N*-oxyl (TEMPOLE) in aqueous solution by (i) sodium ascorbate (for second kinetics) [1–3] and (ii) sodium dithionite (for millisecond kinetics) [4].

Reaction assays were applied under conditions of pseudo-first order kinetics with an excess concentration of the reductant (dithionite or ascorbate) over TEMPOLE so that exponential decays result, and the rate of the reaction can easily be set by the choice of the concentration of the excess reagent.

Optimizations of SF parameters of the driving unit (shot volume and flow rate) as well as of EPR time-sweep acquisition (field position, modulation width, sweep time, and time constant) were performed in the time range from seconds to submilliseconds with the two systems mentioned above. Examples of time-profiles of a complete SF operational cycle "shooting profile" are shown in Fig. 4a for TEMPOLE/ascorbate and in Fig. 4b for TEMPOLE/dithionite. The position of the

H_0 field is fixed at the maximum of the first derivative of the low field line of TEMPOLE (see inset in Fig. 4a) for both systems, and the field modulation is chosen for a maximal EPR amplitude. Time sweep and time constant are adapted to the expected half-life of the (decay) kinetics. The time-sweep display of the SF cycle (EPR amplitude trace **A**) is started by a trigger signal from the driving unit. During a delay time (600 ms in Fig. 4a and 20 ms in Fig. 4b) a zero EPR signal (reduced TEMPOLE from the previous cycle) appears until the hard-stop valve opens and the driving unit starts the flow. Then, an acceleration phase (filling of the cuvette) follows while the EPR signal **A** increases and reaches a stationary level where the supplied fresh reactants and the decay are in a steady-state equilibrium (continuous-flow condition). After the programmed shot time, the driving unit stops the flow and the hard-stop valve closes. After the fast stop of the flowing reaction mixture in the EPR cuvette the reaction proceeds and its rate is visualized by the decay of the EPR signal **A**. When the reaction is completed the SF cycle ends, and the kinetic plot together with the entire shooting profile is stored in the fast acquisition channel of the EPR spectrometer and displayed on screen. The start of the time-swept acquisition is triggered by the driving unit optionally either for the entire profile by the start of flow (including a delay time) (Fig. 4a and b), or for the kinetic display only by the closing of the hard-stop valve (Fig. 6b).

Both examples of the kinetic display and the shooting profile in Fig. 4a and b, which were recorded under different experimental conditions, show the operation of the SF accessory with EPR detection. The following results were obtained:

(i) The time profiles demonstrate the proper settings of shot volume and flow rate for attaining the maximum steady-state signal amplitude before the flow stops and the kinetic decay starts.
(ii) The signal decay exhibits pseudo-first-order kinetics and can be properly fitted by a single exponential curve.
(iii) During the flow and after stopping the flow by the hard-stop valve almost no microphonic disturbances (increased noise or additional peaks) are noticeable on the kinetic displays. This result is—beside a high time resolution—an essential feature of the quality of a SF accessory, particularly under conditions of sensitive EPR detection.

3.3. Time resolution

From geometrical data of the mixer/resonator unit and the maximum flow-rate of 5 ml/s a dead time of 0.28 ms was derived (see Section 2.3.1). This value needs to be verified in experiments with fast reactions. A reaction of 3 mM TEMPOLE and 500 mM dithionite was used with a half-decay time of 0.9 ms being near to the expected time resolution of the instrument. The continuous-flow EPR amplitude (A) during the flow has been measured at various flow-rates, similarly as described in [4]. Fig. 5 shows the plot of A versus the reciprocal flow-rate ($1/v$). From the extrapolation of the linear dependence to the initial amplitude (A_0) at infinite rate, the amplitude A' for the fastest rate ($v = 5$ ml/s), and the measured half-decay time of the reaction, the age of the reaction mixture in the EPR active volume (dead-time t_d) have been estimated according to the equation given in Fig. 5.

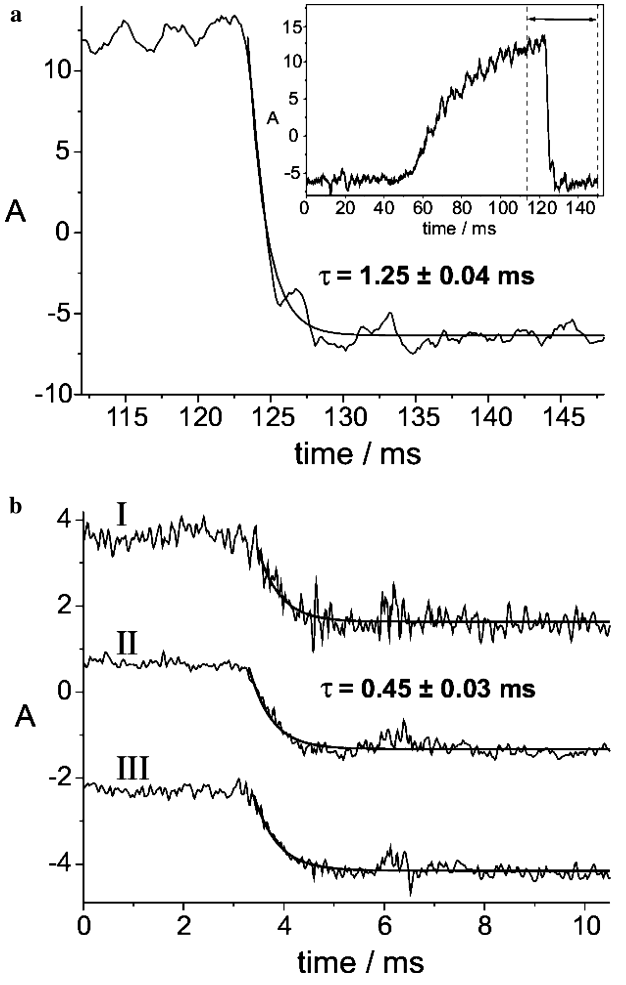

Fig. 6. Time resolution of the EPR stopped-flow apparatus and kinetic displays of fast reactions. The decay has been fitted with a single exponential (bold line), the resulting relaxation time τ (the inverse of the reaction rate) is given. (a) TEMPOLE (3 mM) + dithionite (500 mM), pH 5.0. Inset: complete stopped-flow cycle. EPR: 345.8 mT, 0.7 mT (50 kHz), 10 mW, scan time: 154 ms, time constant: 0.64 ms; flow: 2 × 120 μl, 2.0 ml/s, no delay time. (b) TEMPOLE (3 mM) + dithionite (1 M), pH 5.0. The acquisition starts 3 ms before the hard-stop valve closes. (I) Single shot, (II) accumulation of 6 shots (divided by 6), (III) addition of 4 single shots (divided by 4); EPR: 345.4 mT, 0.7 mT (50 kHz), 10 mW, scan time: 20 ms, time constant: 0.04 ms; flow: 2 × 120 μl, 3.0 ml/s.

The evaluation yielded a dead-time $t_d = 0.33$ ms, and a dead-volume $V_d = 1.6$ μl ($V_d = t_d \cdot v$). The experimental values for both, t_d and V_d (relative error is about 10%), are in excellent agreement with those estimated from geometrical data (0.28 ms and 1.4 μl, respectively). Thus, the measured time resolution of the EPR-SF apparatus is 330 μs.

Fig. 6a shows the result of a SF experiment, the kinetic display and the shooting profile (Inset of Fig. 6a), in the millisecond range. In Fig. 6b, a kinetic display is shown after mixing of 3 mM TEMPOLE with 1 M dithionite at pH 5. The fit of the experimental plot results in a relaxation time (the inverse of the reaction rate) of 0.45 ± 0.03 ms for the decay close to the limit of time resolution.[2] Additionally, Fig. 6b demonstrates that the accumulation of six shots (trace II) and the addition of four single shots (trace III) yield identical time evolutions compared with a single shot (trace I) with regard to amplitude (after normalization) as well as signal decay. This shows the high reproducibility of the whole SF system including software, electronics, and control of the stepping motor movements.

4. Summary and outlook

The EPR-SF accessory described in this paper represents a technical improvement as compared with previous instruments listed in Table 1. The novel aspects concern in particular the driving unit of liquid flow as well as the resonator of the EPR detection system.

4.1. Driving unit of reactants

The MIXCON driving unit can optionally be utilized for *two* different fast flow techniques, freeze-quenching sample preparation (off-line with the EPR spectrometer) and EPR-SF experiments (on-line with the EPR spectrometer). A hard-stop valve is installed to set an exact time-zero for the kinetics, which improves the quality of the kinetic plot. The PC-based software package for EPR-SF operation controls essential parameters of the driving unit and the triggering of kinetic displays. The two liquid reactants can be thermostated.

4.2. EPR detection system

The dielectric ring resonator for X-band cw-EPR was designed especially for a high Q factor, small sample volume, high EPR sensitivity for fast flowing aqueous solutions, and small consumption of substances. The small-sized Berger ball mixer combines the advantages of an optimal mixing efficiency and a close distance to the dielectric resonator. The measured high time-resolution of 330 μs of the entire SF accessory is achieved primarily by this closest possible distance between the mixer and the EPR-active volume. The coupling of the dielectric resonator can be fine-tuned by a microwave slide screw tuner in the waveguide line distant from the resonator. Thus, movable parts near the resonator that may cause microphonics are avoided. The compact assembly of all parts of the resonator and the mixer including their pressure-resistant construction enables sensitive EPR measurements with very low microphonic disturbances under SF conditions with variable high pressure. The kinetic plot is displayed as EPR time-sweep in the rapid acquisition channel of an X-band cw-EPR spectrometer, in our case an ESP 300E from BRUKER.

Due to the high technical level of hardware and software of the driving unit, and the design of the EPR detection system being tailored for SF conditions, the EPR-SF accessory proved to be versatile and very reliable. The reproducibility of the data obtained during operation is high and allows accumulation of kinetic plots in the millisecond region. Performance tests of the EPR-SF accessory with two different radical reactions have resulted in kinetic plots of very high quality.

The described EPR-SF apparatus could advantageously be applied to study local dynamics of spin-labelled proteins, a rapidly growing field of biological EPR applications. We will use the EPR-SF technique in future experiments to investigate rates of redox reactions of paramagnetic centers in radical enzymes which are EPR-observable at room temperature in the liquid state, e.g., rate constants for oxidation of a copper complex, a model for galactose oxidase, to discriminate metal oxidation from the generation of ligand radicals. The EPR-SF technique will also be applied to compare rate constants of the reaction (inactivation) of the functional essential tyrosine radical in ribonucleotide reductase from *Mycobacterium tuberculosis* (R2 protein) by various reducing inhibitor-based agents, which are considered as possible antibiotics against tuberculosis.

Acknowledgments

The authors appreciate the excellent cooperation with Dr. Yves Dupont and Dr. Tobias Henzler from the Bio-Logic Company in Grenoble, France, at adaptation of the freeze-quenching MIXCON apparatus and the hard-stop valve to EPR-SF operation. We are grateful to Dr. Roger Isaacson from Department of Physics, University of California, San Diego, USA, for the generous gift of the dielectric ceramic rings; to Dr. Andrzej Sienkiewicz from Polytechnical University in Lausanne, Switzerland, and Institute of Physics, Polish Academy of

[2] It is also possible that this number is the closing time of the stop valve, but the clear exponential decay suggests that it is rather the inverse rate of the reaction.

Sciences, Warsaw, for helpful discussions on designing the resonator/mixer assembly; and to Dipl.-Ing. Holger Lassmann from the paper machine company (PAMA) in Freiberg, Germany, for critical and helpful discussion about O-ring sealings. Particular thank is directed to the team of the workshop of the MPI for Bioinorganic Chemistry in Mülheim for skillful fine mechanical work of the dielectric resonator, and Frank Reikowski and Gudrun Klihm for technical assistance at microwave measurements and testing the entire instrument with the EPR spectrometer. We thank the quartz factory in Ilmenau, Germany, for providing samples for EPR quartz cuvettes.

This work was supported by the Deutsche Forschungs-Gemeinschaft (DF6) grant SCHM 1676/1-1 and by the Max-Planck Society, Germany.

References

[1] W. Hubbel, W. Froncisz, J. Hyde, Continuous and stopped-flow EPR spectrometer based on a loop gap resonator, Rev. Sci. Instrum. 58 (1987) 1879–1886.
[2] A. Sienkiewicz, K. Qu, C.P. Scholes, Dielectric resonator-based stopped-flow electron paramagnetic resonance, Rev. Sci. Instrum. 65 (1994) 68–74.
[3] A. Sienkiewicz, A. daCosta Ferreira, B. Danner, C.P. Scholes, Dielectric resonator-based flow and stopped-flow EPR with rapid field scanning: a methodology for increasing kinetic information, J. Magn. Res. 136 (1999) 137–142.
[4] V.M. Grigoryants, A.V. Veselov, C.P. Scholes, Variable velocity liquid flow EPR applied to submillisecond protein folding, Biophys. J. 78 (2000) 2702–2708.
[5] N. Klimes, G. Lassmann, B. Ebert, Time-resolved EPR spectroscopy stopped-flow EPR apparatus for biological application, J. Magn. Res. 37 (1980) 53–59.
[6] J. Jiang, J.F. Bank, W. Zhao, C.P. Scholes, The method of time-resolved spin-probe oximetry: its application to oxygen consumption by cytochrome oxidase, Biochemistry 31 (1992) 1331–1339.
[7] J. Jiang, J.F. Bank, C.P. Scholes, Subsecond time-resolved spin-trapping followed by stopped-flow EPR of Fenton products, J. Am. Chem. Soc. 115 (1993) 4742–4746.
[8] G. Lassmann, L. Thelander, A. Gräslund, EPR stopped-flow studies of the reaction of tyrosyl radicals of protein R2 from ribonucleotide reductase with hydroxyurea, Biochem. Biophys. Res. Commun. 188 (1992) 879–887.
[9] S. Pötsch, M. Sahlin, Y. Langelier, A. Gräslund, G. Lassmann, Reduction of the tyrosyl radical and the iron-center in protein R2 ribonucleotide reductase from mouse, herpes-simplex-virus, and *E. coli* by *p*-alkoxyphenols, FEBS Lett. 374 (1995) 95–99.
[10] M. Sahlin, G. Lassmann, S. Pötsch, B.M. Sjöberg, A. Gräslund, Transient free radicals in iron/oxygen reconstitution of mutant protein R2 Y122F. Possible participants in electron transfer chains in ribonucleotide reductase, J. Biol. Chem. 270 (1995) 12361–12372.
[11] K. Qu, J.L. Vaughn, A. Sienkiewicz, C.P. Scholes, J.S. Fetrow, Kinetics and motional dynamics of spin-labeled yeast iso-1-cytochrome *c*: stopped-flow EPR as a probe for protein folding/unfolding of the C-terminal helix spin-labeled at cysteine102, Biochemistry 36 (1997) 2884–2897.
[12] K. DeWeerd, V.M. Grigoryants, Y. Sun, J.S. Fetrow, C.P. Scholes, EPR-detected folding kinetics of externally located cysteine-directed mutants of iso-1-cytochrome *c*, Biochemistry 40 (2001) 15846–15855.
[13] U. Marx, G. Lassmann, K. Wimalasena, P. Müller, A. Herrmann, Rapid kinetics of insertion and accessibility of spin-labelled phospholipid analogs in lipid membranes: a stopped-flow electron paramagnetic resonance approach, Biophys. J. 73 (1997) 1645–1654.
[14] U. Marx, G. Lassmann, H.G. Holzhütter, D. Wüstner, A. Höhlig, J. Kubelt, P. Müller, A. Herrmann, Rapid flip-flop of phospholipids in endoplasmatic reticulum membranes studied by a stopped-flow approach, Biophys. J. 78 (2000) 2628–2640.
[15] J. Stach, R. Kirmse, W. Dietsch, G. Lassmann, V.K. Belyaeva, I.N. Marov, Ligand exchange reactions between copper(II)-and nickel(II)-chelates of different sulfur- and selenium-containing ligands. Kinetics of ligand exchange reactions studied by stopped-flow-ESR, Inorg. Chim. Acta 96 (1985) 55–59.
[16] Q.H. Gibson, Apparatus for the study of rapid reactions, J. Physiol. 117 (1952) P49–P50.
[17] I. Yamazaki, H.S. Mason, L. Piette, Identification, by electron paramagnetic resonance spectroscopy, of free radicals generated from substrate of peroxidase, J. Biol. Chem. 235 (1960) 2444–2449.
[18] M. Jaworski, A. Sienkiewicz, C.P. Scholes, Double-stacked dielectric resonator for sensitive EPR measurements, J. Magn. Res. 124 (1997) 87–96.
[19] S.M. Bromberg, I.Y. Chan, Enhanced sensitivity for high-pressure EPR using dielectric resonators, Rev. Sci. Instrum. 63 (1992) 3670–3673.
[20] R.W. Dykstra, G.D. Markham, A dielectric sample resonator design for enhanced sensitivity of EPR spectroscopy, J. Magn. Reson. 69 (1986) 350–355.
[21] W.M. Walsh Jr., L.P. Rupp Jr., Enhanced ESR sensitivity using a dielectric resonator, Rev. Sci. Instrum. 57 (1986) 2278–2279.
[22] R.L. Berger, B. Balko, H.F. Chapman, High resolution mixer for the study of the kinetics of rapid reactions in solution, Rev. Sci. Instrum. 39 (1968) 493–498.
[23] R.L. Berger, B. Balko, W. Borcherdt, W. Friauf, High speed optical stopped-flow apparatus, Rev. Sci. Instrum. 39 (1968) 486–493.
[24] P.W. Atkins, A. Horsfield, M.C.R. Symons, Oxides and oxyions of the non-metals, Part VII, $SO_2^- + ClO_2$, J. Chem. Soc. (1964) 5220–5225.